Received: May 25, 2016 Revised: September 11, 2016 Accepted: September 28, 2016

(onlinelibrary.wiley.com) DOI: 10.1111/ner.12541

Optimization of Transcutaneous Vagus Nerve Stimulation Using Functional MRI

Natalia Yakunina, PhD*†; Sam Soo Kim, MD, PhD†‡; Eui-Cheol Nam, MD, PhD†§

Objective/Hypothesis: Vagus nerve stimulation (VNS) is an established therapy for drug-resistant epilepsy, depression, and a number of other disorders. Transcutaneous stimulation of the auricular branch of the vagus nerve (tVNS) has been considered as a non-invasive alternative. Several functional magnetic resonance imaging (fMRI) studies on the effects of tVNS used different stimulation parameters and locations in the ear, which makes it difficult to determine the optimal tVNS methodology. The present study used fMRI to determine the most effective location for tVNS.

Materials and Methods: Four stimulation locations in the ear were compared: the inner tragus, inferoposterior wall of the ear canal, cymba conchae, and earlobe (sham). Thirty-seven healthy subjects underwent two 6-min tVNS stimulation runs per electrode location (monophasic rectangular 500 μs pulses, 25 Hz). General linear model was performed using SPM; region-of-interest analyses were performed for the brainstem areas.

Results: Stimulation at the ear canal resulted in the weakest activation of the nucleus of solitary tract (NTS), the recipient of most afferent vagal projections, and of the locus coeruleus (LC), a brainstem nucleus that receives direct input from the NTS. Stimulation of the inner tragus and cymba conchae activated these two nuclei as compared to sham. However, ROI analysis showed that only stimulation of the cymba conchae produced a significantly stronger activation in both the NTS and LC than did the sham stimulation.

Conclusions: These findings suggest that tVNS at the cymba conchae properly activates the vagal pathway and results in its strongest activation, and thus may be the optimal location for tVNS therapies applied to the auricle.

Keywords: Auricular branch of vagus nerve, functional magnetic resonance imaging, locus coeruleus, nucleus of solitary tract, transcutaneous vagus nerve stimulation

Conflict of Interest: The authors reported no conflict of interest.

INTRODUCTION

Vagus nerve stimulation (VNS) is an approved treatment for epilepsy, as well as a therapeutic option for a wide variety of disorders, including depression, anxiety, and Alzheimer's disease (1–5). This technique is implemented by surgically implanting a stimulator on the chest wall and running a wire from the stimulator to the vagus nerve in the neck. VNS triggers the release of several neuromodulators that are thought to enhance plastic changes in the cerebral cortex (6,7); when paired with motor or sensory stimuli, it promotes a substantial reorganization of cortical maps (8–10). Recently, a rat model was used to demonstrate that VNS paired with tones reverses tinnitus-related plasticity of the auditory cortex (11). Existing theories on the underlying mechanisms of VNS therapy include, among others, the modulation of norepinephrine release via projections extending from the nucleus of solitary tract (NTS) to the locus coeruleus (LC), which subsequently influence the limbic, reticular, and autonomic centers of the brain (12–14).

Although the clinical efficacy of VNS is well recognized, the adverse effects related to its invasiveness make it a difficult, risky, and expensive method for large-scale application to clinical populations. To minimize these negative aspects, transcutaneous stimulation of the afferent auricular branch of the vagus nerve (ABVN) at the external ear has been considered as an alternative treatment option (15). Currently, several commercial transcutaneous VNS (tVNS) devices are available, including NEMOS® (http://www.cerbomed.com), which stimulates the cymba conchae for the treatment of epilepsy, P-stim® (http://www.octusaspine.com/p-stim.html), which stimulates three acupunctural points in the auricle for the management of

Address correspondence to: Eui-Cheol Nam, MD, PhD, Department of Otolaryngology, School of Medicine, Kangwon National University, 1 Kangwondaehak-gil, Chuncheon 200-701, Kangwon-do, Republic of Korea. Email: birdynec@kangwon.ac.kr

* Institute of Medical Science, School of Medicine, Kangwon National University, Kangwondaehak-gil 1, Chuncheon, Republic of Korea;
† Neuroscience Research Institute, Kangwon National University Hospital, Baengnyeong-ro 156, Chuncheon, Republic of Korea;
‡ Department of Radiology, School of Medicine, Kangwon National University, Kangwondaehak-gil 1, Chuncheon, Republic of Korea; and
§ Department of Otolaryngology, School of Medicine, Kangwon National University, Kangwondaehak-gil 1, Chuncheon, Republic of Korea

For more information on author guidelines, an explanation of our peer review process, and conflict of interest informed consent policies, please go to http://www.wiley.com/WileyCDA/Section/id-301854.html

Source(s) of financial support: This research was supported by the Basic Science Research Program through the National Research Foundation of Korea (NRF) and was funded by the Ministry of Education (2014R1A1A4A01003909).

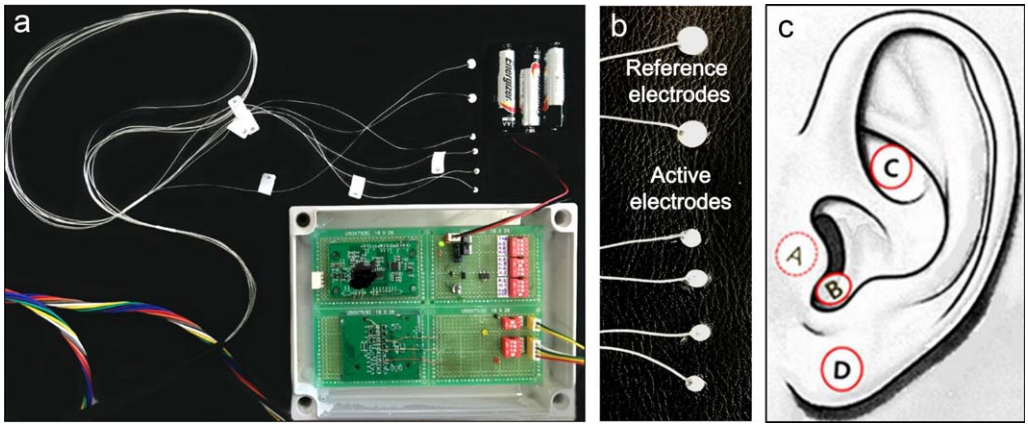

Figure 1. a. Custom-built MRI-compatible tVNS stimulator used in the present study. b. Six silver electrodes (four active, two reference electrodes). c. tVNS stimulation locations: A: inner surface of the tragus, B: inferoposterior wall of the external acoustic meatus, C: cymba conchae, D: earlobe. The reference electrode for locations A, B, and C was placed on the outer wall of the tragus, and the reference electrode for D was placed on the back side of the earlobe.

chronic pain, SaluStim® (http://www.tinnitustreatmentcentre.com), which is designed to relieve tinnitus by applying tVNS at the inner side of the tragus in combination with sound therapy, and gammaCore©, which stimulates the vagus nerve in the neck to relieve pain and reduce headache and migraine (http://gammacore.com). To date, four studies have used functional magnetic resonance imaging (fMRI) to investigate the brain response to tVNS (16–19). However, there are considerable discrepancies among the results of these tVNS fMRI studies. Only two of these studies reported activity in the NTS, which is the primary brain region receiving projections from the vagus nerve (17,19,20). Differences in the study methodologies and the areas of the external ear that were stimulated may have led to variability among the results. As a result, the precise location at which tVNS stimulation would yield the results most specific to vagal stimulation remains unclear.

Thus, the present study employed fMRI to compare the effects of tVNS applied at four different locations in the left ear to identify the most effective location for tVNS therapy in the auricle. Three locations were selected for stimulation based on existing knowledge regarding the anatomical distribution of the ABVN (21–24), previous tVNS fMRI studies (16–19), and the stimulation locations for commercially available tVNS devices: the inner surface of the tragus, the inferoposterior wall of the external acoustic meatus (ear canal), and the cymba conchae. Furthermore, stimulation at the earlobe, which is known to be relatively free of vagal innervation, was performed as a sham stimulation (21).

METHODS

Subjects

The present study included 37 healthy individuals with a mean age of 30.9 ± 8.2 years (two left-handed subjects, 18 males). The Institutional Review Board of Kangwon National University Hospital approved the study protocol, and all subjects provided written informed consent prior to participation. The subjects had no known otological, neurological, or psychological disorders and were not taking any medications at the time of experiment. Prior to the study, the stimulation procedure and the experiment protocol were explained to subjects, who were informed that they could leave the experiment at any time. Prior to fMRI scanning session, subjects were familiarized with the electrical stimulation through preliminary sensory/pain threshold testing (described below), which lasted about 20 min.

Electrical Stimulation

All electrical stimulation was applied using a custom-made stimulator (Fig. 1a) connected with silver wires to six electrodes (four stimulation and two reference electrodes; Fig. 1b). The electrodes were 99.99% pure silver, and the connecting 10-m cables were designed for MRI compatibility and did not generate any MRI artifacts. The electrical stimulus was a monophasic rectangular impulse with a pulse width of 500 μsec and a stimulation frequency of 25 Hz, which was shown to produce better results than low frequencies during VNS (25). The stimulation was performed at the left ear because the efferent vagal fibers to the heart are generally located on the right side (13). The electrodes for the tVNS were positioned at four locations in the left ear: electrode A was at the inner surface of the tragus, electrode B was at the inferoposterior wall of the ear canal (at the cartilaginous part of the ear canal), electrode C was at the cymba conchae, and electrode D was at the earlobe (Fig. 1c). The reference electrode for electrodes A, B, and C were placed at the outer surface of the tragus, whereas the reference electrode for electrode D (sham) was placed at the backside of the earlobe.

Prior to starting the scanning session, the subjects' sensory and pain thresholds were tested outside of the scanner room to familiarize them with the stimulation sensation and procedure. This testing was conducted at every stimulation location after the electrodes were fixed in the subject's left ear. Starting from 0.1 mA, the intensity was gradually increased by 0.1 mA until the subject reported a sensation (sensory threshold); the intensity was then gradually increased until the subject started to feel pain or intolerable discomfort (pain threshold). The procedure was repeated for each of the four electrodes. After that the subject was placed into the MRI scanner with the electrodes kept in their positions. Prior to each functional run, the sensory and pain thresholds of the subjects were tested again inside the MRI scanner using the above procedure; the determined thresholds were accepted as final. The stimulation intensity for each electrode was chosen as the intensity that was 0.1 mA weaker than the intensity corresponding to the pain threshold. The electrodes were not moved or removed for the entire duration of the scanning procedure, starting from the preliminary testing outside of the scanner room. The subjects were instructed to remain still

with their eyes closed and to concentrate on the sensation. The subjects were supplied with the emergency button in case they needed to interrupt the scanning, and were instructed to feel free to withdraw from the experiment at any moment if continuing the experiment did not feel comfortable. The subjects were asked about their condition throughout the functional session after every run.

Data Acquisition

Imaging was performed using a 3.0 T MRI scanner (Philips Achieva, Philips, Amsterdam, Netherlands) with a 32-channel SENSE head coil (Philips). Coronal 3D T1-weighted high-resolution structural images of the whole brain were acquired for anatomical orientation using the following parameters: TR = 9.8 ms, TE = 4.8 ms, FA = 8°, slice thickness = 1.0 mm, matrix = 256 × 256 × 195, FOV = 220 × 220 mm, and voxel size = 0.94 × 0.94 mm. Additionally, T2*-weighted functional images were acquired using a gradient echo planar imaging (EPI) sequence with the following parameters: 30 oblique coronal slices, TR = 2000 ms, TE = 35 ms, FA = 90°, matrix = 80 × 80, FOV = 220 × 220 mm, and voxel size = 2.75 × 2.75 mm. The slice plane was positioned parallel to the back wall of the brainstem. Each location was stimulated in two runs with 30 sec of stimulation followed by 1 min of rest; this cycle was repeated four times in a run. Each subject underwent eight 6-min fMRI runs total, with up to 90 sec of rest in between runs, during which the subjects were asked about subjective strength of experienced sensation and their overall condition. The order of stimulation was counterbalanced and varied from subject to subject. A total of 360 functional volumes were obtained for each stimulation location. The stimulus intensity was adjusted individually for each electrode before each scan to the level of a prominent but bearable sensation immediately below the subjective pain threshold for each subject.

Throughout the entire imaging session, the heart rate of each subject was monitored using a wireless MRI-compatible pulse oximeter (Medrad Veris^{TM} 8600, Medrad Inc., Warrendale, PA, USA) attached to the right index finger. The experiment was to terminate immediately if the subject showed bradycardia (heart rate < 60 BPM) or abnormal cardiac rhythms.

Data Analysis

All data were preprocessed and statistically analyzed using the SPM12 software package (Wellcome Department of Cognitive Neurology, Institute of Neurology, University College London, UK) in the MATLAB 7.8 programming environment (MathWorks, Inc.; Natick, MA, USA). Preprocessing included the following steps for each subject: correction for head motion, slice timing correction, coregistration to the first volume of each run, normalization to the standard Montreal Neurological Institute (MNI) T1 template, and spatial smoothing using an 8-mm isotropic Gaussian kernel. Since brainstem nuclei are considerably smaller than cortical areas, smoothing may not be appropriate for brainstem analysis; therefore, to explore brainstem activity, the additional analysis on the unsmoothed data was performed.

At the individual level, the preprocessed data were fitted to a general linear model implemented in SPM12. For each run, the boxcar stimulus function was convolved with a canonical hemodynamic response function and data were high-pass filtered using a cutoff period of 128 sec. Motion parameters were added as nuisance regressors. Serial correlations in the fMRI time series were accounted for using an autoregressive AR(1) model. The blood oxygen level dependent (BOLD) activity in each of the four stimulation locations was first modeled separately to obtain the stimulation–rest contrast for each electrode. Then, the stimulation data for all four locations were fitted into one model and the contrasts A–D, B–D, and C–D were obtained to compare the stimulations in the three active locations (A, B, and C) with that in the sham location (D). One-sample *t*-tests were performed on the resulting individual contrast maps to obtain group activation maps, and these were corrected for multiple comparisons using a cluster-significance threshold of $p < 0.05$ to indicate statistical significance. For the brainstem, the same analysis was done on the unsmoothed data.

Regions-of-interest (ROIs) were defined for the LC and NTS because the NTS receives a majority of the vagal afferent sensory fibers and then sends direct projections to the LC (26–28). The LC ROI was defined using an available template (http://www.eckertlab.org/LC) (29), whereas the NTS ROI was defined based on existing literature (30,31). All statistical analyses were performed using IBM SPSS software (version 19.0; IBM Corp.; Armonk, NY, USA). The percentage signal change (PSC) was calculated using the following formula: $100 \times (S_{stim} - S_{rest})/S_{rest}$, where S_{stim} was the signal intensity during the stimulus periods and S_{rest} was the signal intensity during the resting periods. The number of voxels with $t > 3.33$ for activation and $t < -3.33$ for deactivation, the average t-score, and the PSC were calculated for each ROI for each electrode location using the unsmoothed data, and each of the active locations (A, B, and C) was compared with the sham location (D) using paired t-tests with Bonferroni's correction for multiple comparisons. Stimulation intensities and sensory thresholds were compared among all locations using a within-subject analysis of variance (ANOVA) with Bonferroni's correction for multiple comparisons. Pearson's correlation analysis was used to compare the relationships between the individual stimulation intensities and the PSC for both the LC and NTS ROIs and for each location to determine whether the level of activation and the intensity of stimulation were dependent.

RESULTS

The sensory thresholds at electrodes A, B, C, and D ranged from 0.2–1 mA, 0.1–1.4 mA, 0.1–1.2 mA, and 0.1–1.2 mA, respectively, with means ± standard deviations (SD) of 0.44 ± 0.21, 0.45 ± 0.27, 0.51 ± 0.26, and 0.46 ± 0.22, respectively (Fig. 2). The stimulation intensities at electrodes A, B, C, and D ranged from 0.2–1.8 mA with means ± SD of 0.77 ± 0.42, 0.81 ± 0.48, 0.91 ± 0.47, and 0.81 ± 0.38 mA, respectively. The mean stimulation intensities were similar for all four locations, except for the stimulation at electrode C, which was stronger than that at electrode A ($p < 0.05$, Bonferroni-corrected). No subjects experienced bradycardia (heart rate < 60 BPM) or abnormal cardiac behavior during the course of the experiment. Nobody withdrew or was withdrawn from the experiment.

Comparison of Stimulation Versus Resting States

The group analysis results of the four experimental locations relative to baseline are presented in Table 1. Stimulation at electrodes A and D caused bilateral suprathreshold activation in the supramarginal gyrus, whereas electrode B caused this activation on only the right side. Stimulation at electrodes A and C activated the right thalamus, bilateral stria terminalis, bilateral corpus callosum, and cerebellum. Stimulation at electrode A caused additional lateralized activation in the right anterior insula, frontal and central operculum, and putamen. Additionally, the right frontal gyrus was activated after stimulation at electrodes A (inferior) and D (inferior/middle; Fig. 3). Stimulation at all four electrodes produced deactivation in the auditory and auditory-associated cortices in the superior and

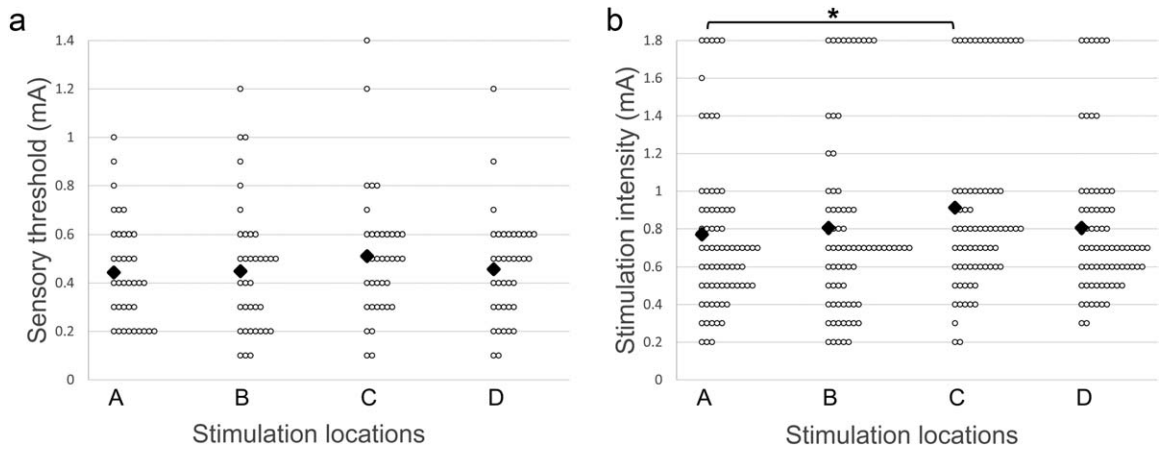

Figure 2. Distributions and average values of the sensory thresholds (a) and stimulation intensities (b) for each location. The mean values are marked with a solid diamond. *: $p < 0.05$ (within-subject ANOVA, Bonferroni-corrected for multiple comparisons).

middle temporal gyri (A, B, and C bilaterally and D on the right side). Electrode A deactivated the bilateral inferior temporal gyri and left planum temporale, whereas electrode C deactivated only the left planum temporale.

In the limbic system, deactivation was observed in the posterior cingulate gyrus and hippocampus for all electrode locations, in the amygdala for electrodes B and C, in the posterior insula for electrodes A and C, and in the parahippocampal gyrus for electrodes A, B, and C. Deactivation was also observed in a number of frontal and occipital regions including the precuneus, occipital, lingual, fusiform, middle/anterior cingulate, and middle/superior frontal gyri (Table 1, Fig. 3). When the threshold was lowered to $p < 0.05$, uncorrected for multiple comparisons, the bilateral LC and NTS could be seen on the activation maps of electrodes A and C, whereas the activation map for electrode B showed only the NTS, and the activation map for electrode D did not show either of these brainstem nuclei (Fig. 4).

The unsmoothed data analysis showed the LC activation for the electrodes A, B, and C (bilateral for A and C and unilateral for B), and the bilateral NTS for the same three electrodes, uncorrected for multiple comparisons ($p < 0.001$). Neither the LC nor the NTS was observed on the activation map for the electrode D (Fig. 5a).

Comparisons of Active Location Stimulations (A, B, and C) With the Sham Stimulation (D)

Compared with the sham earlobe stimulation (D), electrode B did not produce any results above the chosen threshold, whereas electrodes A and C resulted in increased activity in the LC and cerebellum (Fig. 6a), and electrode A showed greater activity in the thalamus and putamen. When examining the uncorrected maps of the differences versus the sham stimulation ($p < 0.001$), additional activations of the NTS, thalamus, and caudate nucleus were observed on both the A–D and C–D maps (Fig. 6b). However, the B–D contrast did not display any activity, even with the uncorrected threshold.

In the analysis using the unsmoothed data, A–D and C–D contrast maps showed the bilateral LC and NTS activations, while B-D contrast displayed only the unilateral LC (Fig. 5b). Furthermore, NTS activation was observed on the individual maps of the following numbers of subjects per contrast: A (9 subjects), B (11 subjects), C (14 subjects), A–D (12 subjects), B–D (5 subjects), and C–D (16 subjects).

ROI Analysis

Electrodes A and C had a significantly greater number of activated voxels above the chosen threshold and higher t-scores than electrode D for the NTS (Fig. 7). For the LC, only the electrode C had a significantly higher t-scores than electrode D. All absolute correlations between stimulation intensity and the PSC were less than 0.2, and none was significant for either the LC or NTS.

DISCUSSION

Four previous studies have investigated the effects of tVNS using fMRI, but several different areas of the ear were stimulated; namely, the inner wall of the tragus (16–18), the posterior side of the ear canal (17), and the cymba conchae (19). Similar to the present study, Kraus et al. (2013) compared stimulation at the inner tragus and posterior wall of the ear canal with sham stimulation at the earlobe. However, the cymba conchae, which is one of the major ABNV-innervated locations that has been previously studied and is the location used by the commercial device NEMOS®, was not included in that study. Additionally, it has been suggested that the inferoposterior wall, rather than the posterior wall, is the aspect of the ear canal most heavily innervated by the vagus (22,24). The most commonly observed areas in these tVNS fMRI studies, including the insula, amygdala, hippocampus, parahippocampal gyrus, thalamus, cerebellum, cingulate gyrus, and frontal and paracentral lobules, generally coincided with the findings of previous VNS fMRI studies (25,32–36), although the activated and deactivated areas were not entirely consistent among these studies.

The NTS is the primary brainstem target of the vagus, as it receives approximately 95% of all vagal afferents (12,26). The NTS projects to numerous areas in forebrain, limbic, and brainstem structures (17,19,20) including the LC, which is the major noradrenergic nucleus in the brain and plays a key role in the mechanisms of action underlying VNS (27,28,37,38). It is difficult to determine activation in small brainstem structures such as these due to their locations in the brainstem and small sizes, which weaken signal intensity due to a greater number of motion artifacts after vascular fluctuation (39). Nevertheless, activation in both of these structures was determined in the present study. Only two studies have previously succeeded in demonstrating this type of activation (17,19), whereas another study reported only ipsilateral LC activation (18). In the

Table 1. The Present and Previous fMRI Studies Using VNS and tVNS.

First author	Bohning	Lomarev	Narayanan	Sucholeiki	Liu	Mu	Nahas
Procedure used	VNS	VNS	VNS	VNS	VNS	VNS	VNS
Year of publication	2001	2002	2002	2002	2003	2004	2007
Number of subjects	9 sub	9 sub	5 sub	4 sub	5 sub	12 sub	17 sub
Statistical threshold	$p < 0.001$ uncorrected	$p < 0.001$ uncorrected	individual	individual	individual	$p<0.001$, cluster $p<0.05$	$p<0.1$
Contrast (tVNS)							
Analysis method (tVNS)							
Locus coeruleus							
Nucleus of solitary tract							
Amygdala	↑ l						
Angular gyrus							
Bed nucleus of stria terminalis							
Caudate						↑ l	
Cerebellar hemisphere					↑ b	↓ r	↑ b
Cingulate gyrus anterior						↓ r	
Cingulate gyrus middle							
Cingulate gyrus posterior						↓ b	↓ r
Corpus callosum							
Frontal gyrus inferior				↑ b	↑ r		
Frontal gyrus middle				↑ b			
Frontal gyrus superior		↑ r	↑ l	↑ b			
Fusiform gyrus							↓ l
Hippocampus						↓ l	
Hypothalamus	↑ b	↑ b					
Insula anterior			↑ b				
Insula posterior			↑ b			↑ l	
Occipital gyrus inferior	↑ b		↑ b	↑ b (not all)	↑ b		
Occipital gyrus middle							
Occipital gyrus superior		↓ b					
Parahippocampal gyrus						↓ r	
Parietal lobe					↑ b		
Postcentral gyrus			↑ l			↓ r	
Precentral gyrus						↑ l	
Precuneus							
Putamen						↑ l	
Stria terminalis							
Supramarginal gyrus							↑ l
Temporal gyrus inferior							↓ r
Temporal gyrus middle	↑ l				↑ r	↑ l	↓ r
Temporal gyrus superior			↑ r	↑ l	↑ b		↑ b
Thalamus			↑ b				

present study, stimulation at electrodes A (inner tragus) and C (cymba conchae) produced a greater degree of activation in the NTS and LC compared with the sham (Figs. 5b and 6b), whereas stimulation at electrode B (ear canal) did not. Although electrode A displayed a higher average t-score and number of activated voxels in the NTS compared with electrode D (sham), electrode C was the only location that showed a significantly higher average t-scores in both the LC and NTS compared with the sham (Fig. 7).

The notably weak NTS activation produced by electrode B may indicate that there was an insufficient stimulation of the ABVN at this location, probably due to a high degree of inter-subject variability regarding the ABVN location in the ear canal. Although the cough reflex (Arnold's reflex), which is induced by the mechanical stimulation of the ABVN, is consistently evoked by touching the inferoposterior wall of the ear canal, the ABVN location inside of the ear canal appears quite variable among subjects (21–23).

Decreased synaptic activity within the limbic system is one component underlying the VNS mechanisms for the treatment of epilepsy and depression. Limbic system deactivation and decreased regional cerebral blood flow (rCBF) have consistently been shown by fMRI tVNS studies (16,17), and positron emission tomography and single-photon emission computed tomography VNS studies (40–44). In the present study, several major areas of the limbic system were deactivated: the hippocampus and posterior cingulate gyrus were deactivated by electrodes A, B, and C, whereas the parahippocampal gyrus and amygdala were deactivated by electrodes B and C (Table 1, Fig. 3). However, the sham stimulation of electrode D (earlobe) also deactivated these limbic areas. Electrical stimulation

Table 1. *Continued*

First author	Dietrich	Kraus	Kraus		Frangos			
Procedure used	tVNS	tVNS	tVNS		tVNS			
Year of publication	2008	2007	2013		2015			
Number of subjects	4 sub	8 sub	16 sub		12 sub			
Statistical threshold	uncorrected	$p < 0.000003$ uncorrected	$p < 0.001$ uncorrected		$p<0.05$ cluster corrected			
Contrast (tVNS)	A>rest	A>rest	B>D		C>rest		C>D	
Analysis method (tVNS)			anterior B	posterior B	mask	whole brain	mask	whole brain
Locus coeruleus	↑ l				↑ b		↑ b	
Nucleus of solitary tract					↑ l		↑ l	
Amygdala		↓ b			↑ r	↑ r	↑ r	↑ r
Angular gyrus								
Bed nucleus of stria terminalis					↑ b	↑ b	↑ b	↑ b
Caudate						↑ r		↑ r
Cerebellar hemisphere	↓ l					↑ b		↑ b
Cingulate gyrus anterior		↑ r	↑ r	↓ l				
Cingulate gyrus middle								
Cingulate gyrus posterior	↑ l	↓ b	↓ l			↑ b		↑ b
Corpus callosum								
Frontal gyrus inferior		↑ l						
Frontal gyrus middle			↑ b	↓ r				
Frontal gyrus superior		↓ b	↑ b	↓ r				
Fusiform gyrus								
Hippocampus		↓ l			↓ b	↓ b	↓ b	↓ b
Hypothalamus					↓ b	↓ b	↓ b	↓ b
Insula anterior								
Insula posterior	↑ l	↑ b	↑ l		↑ b	↑ b	↑ b	↑ b
Occipital gyrus inferior								
Occipital gyrus middle								
Occipital gyrus superior								
Parahippocampal gyrus		↓ b	↓ l	↑l				
Parietal lobe			↑ r					
Postcentral gyrus	↑ b				↑ b	↑ b	↑ b	↑ b
Precentral gyrus		↑ b						
Precuneus		↓ b						
Putamen						↑ r		↑ r
Stria terminalis					↑ b	↑ b	↑ b	↑ b
Supramarginal gyrus								
Temporal gyrus inferior								
Temporal gyrus middle		↓ b						
Temporal gyrus superior		↓ r						
Thalamus	↑ b (l>r)	↑ r	↓ r		↑ b	↑ b	↑ b	↑ b

of the earlobes has long been used as part of a noninvasive transcutaneous brain stimulation technique known as cranial electrotherapy stimulation (CES), which is approved by the Food and Drug Administration (FDA) for the treatment of insomnia, depression, and anxiety (45,46). The earlobe is primarily innervated by the great auricular nerve that originates from the cervical nerve (C2); thus, CES does not stimulate the ABVN (21). Although its working mechanisms are not yet fully understood, CES is thought to modulate the limbic system, reticular activating system, and hypothalamus which, in turn, subsequently trigger the secretion of neurotransmitters and the production of hormones (46,47). fMRI analyses have revealed that CES results in negative BOLD changes (deactivation) in several brain areas, including the precuneus, precentral and postcentral gyri, posterior cingulate gyrus, and occipital cortex (48). These areas were also affected by tVNS in the present and previous fMRI studies (Table 1). Therefore, earlobe stimulation could induce BOLD changes in the limbic system and other areas that are similar to those observed in response to tVNS, but the degree of activation seems to be much weaker than that induced by tVNS.

In the present study, the auditory system was clearly deactivated by all four electrodes. A previous magnetoencephalography study found that tVNS decreases the amplitude of the auditory-evoked N1m response (49); another tVNS study reported ipsilateral deactivation of the auditory cortex (16). However, in the present study, sham stimulation at the earlobe also induced deactivation at Heschl's gyrus and the superior temporal gyrus, even though it was weaker and only on the contralateral side (Fig. 3). The earlobe is innervated by the great auricular nerve, which is a branch of the cervical plexus, contributed to by fibers from the C2 and C3 spinal nerves (21). Additionally, sensory inputs from the face, ears, and neck via cranial nerves V, VII, IX, and X (vagus) and the dorsal spinal root via C2 converge on the medullary somatosensory nucleus, which is a region in

Table 1. *Continued*

First author	Present study					
Procedure used	tVNS					
Year of publication	2016					
Number of subjects	37 sub					
Statistical threshold	$p < 0.001$, cluster $p < 0.05$ FDR					
Contrast (tVNS)	A>rest	B>rest	C>rest	D>rest	A>D	C>D
Analysis method (tVNS)						
Locus coeruleus					b***	b***
Nucleus of solitary tract					b***	b***
Amygdala		↓ b***	↓ b***			
Angular gyrus	↑ r***	↑ r* ↓ l***	↓ l**	↑ l* ↓ r*		
Bed nucleus of stria terminalis						
Caudate					b**	b*
Cerebellar hemisphere	↑ b***		↑ b***	↓ b***	b**	b**
Cingulate gyrus anterior		↓ l***	↓ b***			
Cingulate gyrus middle			↓ b***	↓ b***		
Cingulate gyrus posterior	↓ b***	↓ b***	↓ b***	↓ b***		
Corpus callosum	↑ b*		↑ b*			
Frontal gyrus inferior	↑ r***			↑ r**		
Frontal gyrus middle		↓ l***	↓ r**	↑ r**		
Frontal gyrus superior	↓ l***	↓ l***	↓ b***	↓ b***		
Fusiform gyrus		↓ b***	↓ b***	↓ b***		
Hippocampus	↓ l***	↓ b***	↓ b***	↓ b***		
Hypothalamus					b***	
Insula anterior	↑ r***					
Insula posterior	↓ l***		↓ l***			
Occipital gyrus inferior			↓ l**			
Occipital gyrus middle		↓ l**	↓ b***	↓ r*		
Occipital gyrus superior		↓ l**	↓ l**			
Parahippocampal gyrus		↓ b***	↓ b***	↓ b***		
Parietal lobe						
Postcentral gyrus	↓ l***		↓ b***	↓ b***		
Precentral gyrus	↑ r***, ↓ l***		↓ b***	↓ l***		
Precuneus	↓ b***	↓ b***	↓ b***	↓ b***		
Putamen	↑ r*				b***	
Stria terminalis	↑ b*		↑ b*			
Supramarginal gyrus	↑ b***	↑ r*		↑ r***, ↑ l*		
Temporal gyrus inferior	↓ b***					
Temporal gyrus middle	↓ b***	↓ b***	↓ b**	↓ r*		
Temporal gyrus superior	↓ b***	↓ b***	↓ b**	↓ r*		
Thalamus	↑ r***		↑ r*		b***	

↑: activation, ↓: deactivation, r: right, l: left, b: bilateral. A: inner tragus, B: ear canal, C: cymba conchae, D: earlobe (sham) stimulation, Ant.: anterior, Post.: posterior.
* $p < 0.05$, ** $p < 0.01$, *** $p < 0.001$ (Cluster-Wise Corrected for Multiple Comparisons).

the lower part of the medulla that projects to the ipsilateral dorsal cochlear nucleus (DCN) (50–52). The DCN receives auditory input from the ipsilateral auditory nerve and relays the information further along the central auditory pathway. Numerous animal and human studies have shown that somatosensory inputs alter auditory responses in the DCN (53–57). In fact, it has been argued that the disinhibition of spontaneous DCN activity resulting from abnormal somatosensory input from the medullary somatosensory nucleus might cause somatic tinnitus, which is characterized by a unilateral location on the side of somatic injury with no auditory disorder (51,58). Therefore, the modulated activity in the auditory system observed in the present study may have been due to excessive somatosensory input following stimulation of either the vagus via electrodes A, B, and C or the C2 nerve via electrode D. This may have altered auditory input into the DCN and further influenced spontaneous activity in the auditory cortex.

In general, the results of the present study are consistent with those of previous VNS and tVNS studies (Table 1). However, even though the limbic areas were similarly deactivated by ear canal stimulation (electrode B) and conchae stimulation (electrode C), electrode B failed to sufficiently activate the LC and NTS, which indicates that the vagal pathway was not adequately stimulated at this location. It seems that stimulating the external acoustic canal (electrode B) induced a similar pattern of limbic deactivation by affecting other cranial nerves that innervate the ear canal and not the ABVN. In contrast, electrodes A and C seem to have successfully activated the vagal afferent pathway. Although both of these electrodes activated the LC and NTS, stimulation at electrode C resulted

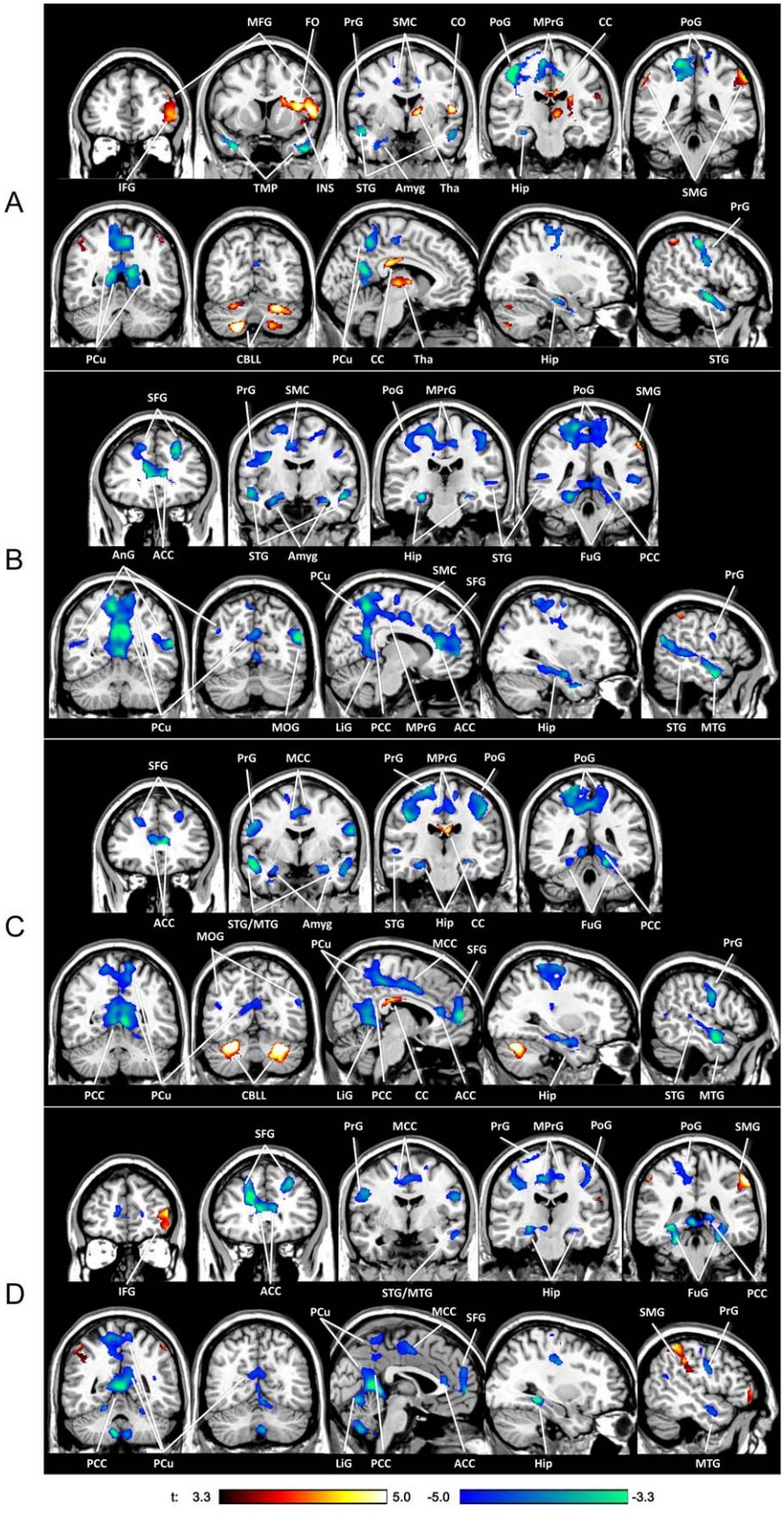

Figure 3. Activations (red) and deactivations (blue) induced by stimulation at electrodes A, B, C, and D ($p < 0.05$, corrected for multiple comparisons). Spatial maps are presented on the most representative sections according to neurological convention. ACC/MCC/PCC: anterior/middle/posterior cingulate cortex, Amyg: amygdala, AnG: angular gyrus, CC: corpus callosum, CBLL: cerebellum, CO/FO: central/frontal operculum, IFG/MFG/SFG: inferior/middle/superior frontal gyrus, Ins: insula, FuG: fusiform gyrus, Hip: hippocampus, LiG: lingual gyrus, MOG: middle orbital gyrus, MPrG: medial precentral gyrus, MTG/STG: middle/superior temporal gyrus, PCu: precuneus, PoG/PrG: postcentral/precentral gyrus, SMC: supplementary motor cortex, SMG: supramarginal gyrus, Tha: thalamus, TMP: temporal pole.

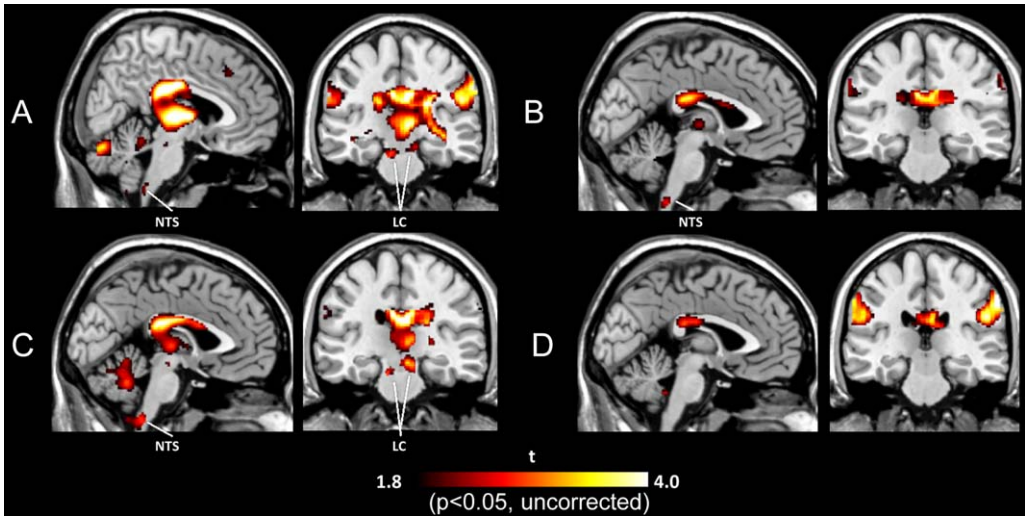

Figure 4. Activation maps for electrodes A, B, C, and D ($p < 0.05$ uncorrected for multiple comparisons). LC: locus coeruleus, NTS: nucleus of solitary tract.

in a significantly greater activation at both nuclei compared with the sham (Fig. 7). Thus, the location of electrode C (cymba conchae) may be a preferred site for future tVNS therapies.

A cadaver study revealed that the inner tragus is solely innervated by the ABVN in 45% of cases (21), which is the reason that this location is common in many tVNS studies. Moreover, this could also explain the successful activation of VNS-related areas following the tVNS at this location that has been observed in previous studies (16,18). On the other hand, the cymba conchae was innervated by the ABVN in 100% of cases, which makes it a more attractive candidate and may have contributed to the fact that the cymba conchae performed better than the inner tragus in terms of stimulating the ABVN in the present study.

Although there was no correlation between stimulation intensity and the PSC in the LC and NTS in the present study, the possibility that the stronger stimulation at electrode C contributed to the outcome relative to electrode A cannot be excluded. In practical terms, this would mean that electrode C (cymba conchae) was capable of receiving a stronger intensity and, thus, may offer an advantage over the inner tragus during long-term tVNS treatment.

The present study has several limitations that should be considered. First, the control location for the sham stimulation (earlobe) was chosen for the present study because a majority of previous tVNS studies (16,17,19) also used this location due to its proximity to other studied vagus-innervated locations and because it is known to be anatomically free of vagal innervation. However, in the present study, stimulation of this location (electrode D) resulted in BOLD changes in brain areas that somewhat overlapped with those stimulated by tVNS. Therefore, clear differences between tVNS and the sham stimulation could not be demonstrated in cortical areas. Second, the four chosen locations were stimulated during a single functional session, which limited the imaging time and, thus, the stimulation duration. To overcome the loss of power due to the shorter stimulation duration and fewer tVNS repetitions, a large

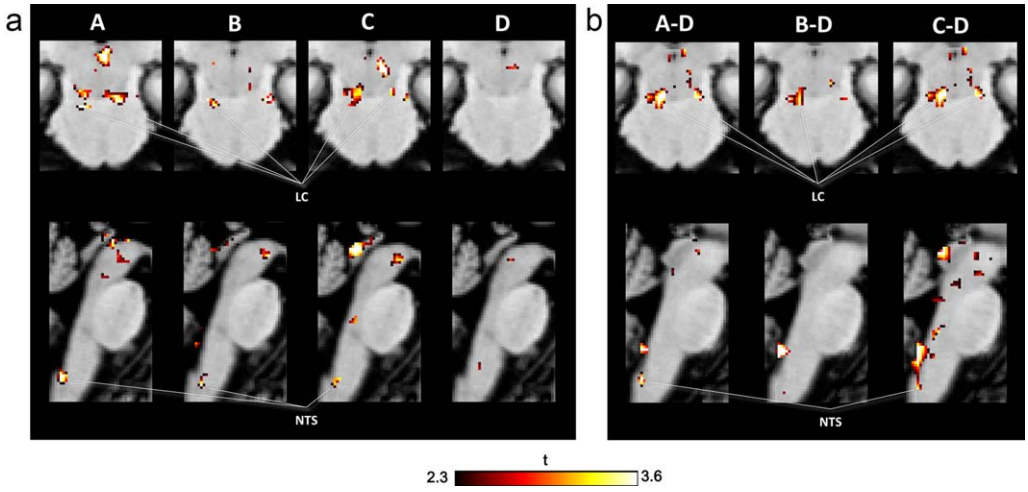

Figure 5. Spatial maps of the GLM analysis in the brainstem using the unsmoothed data. a. Activation maps for electrodes A, B, C, and D. b. Contrast maps of the three active locations versus the sham location. The maps are presented at $p < 0.001$, uncorrected for multiple comparisons. LC: locus coeruleus, NTS: nucleus of solitary tract.

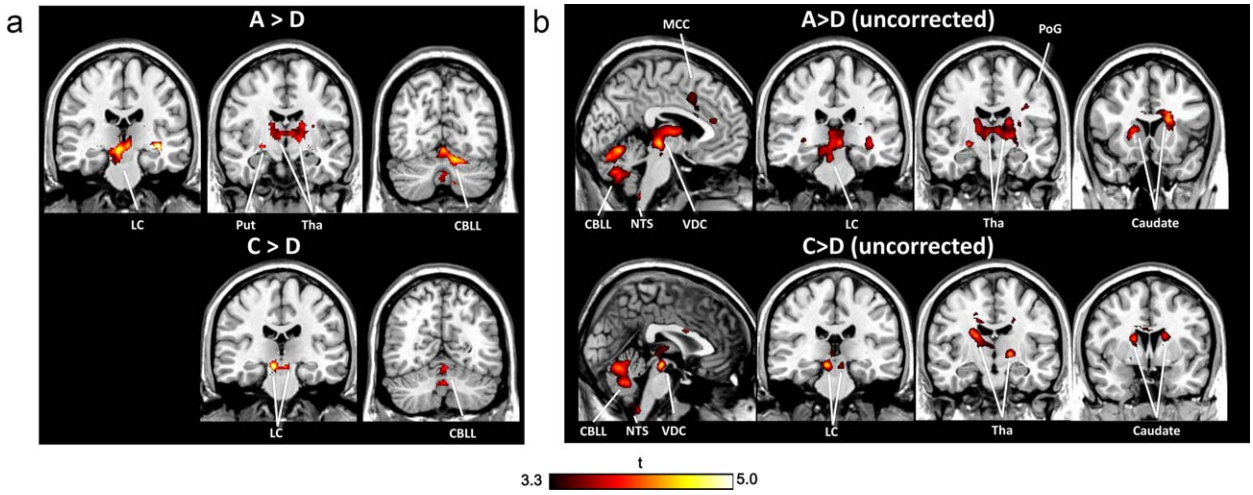

Figure 6. Spatial maps of the differences between the active stimulation locations and the sham stimulation location, corrected (a) and uncorrected (b) for multiple comparisons. Because the results for electrode B did not significantly differ from those for the sham electrode, the data for this location are not presented. CBLL: cerebellum, LC: locus coeruleus, MCC: middle cingulate cortex, NTS: nucleus of solitary tract, PoG: postcentral gyrus, Put: putamen, Tha: thalamus, VDC: ventral diencephalon.

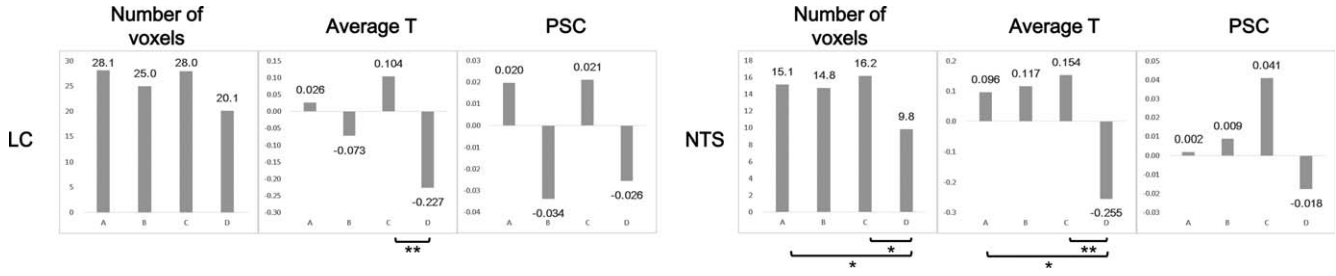

Figure 7. Results of the voxel-wise analysis: number of voxels, average t-value, and PSC in the LC and NTS for each electrode location. *: $p < 0.05$, **: $p < 0.01$ (paired t-test, Bonferroni-corrected for multiple comparisons). The horizontal axis depicts the stimulation locations. LC: locus coeruleus, NTS: nucleus of solitary tract, PCS: percentage signal change.

number of subjects were recruited. It should also be noted that the present study explored locations for tVNS in the ear and not the neck, so our conclusions are limited to the auricular tVNS.

CONCLUSIONS

The present results suggest that the cymba conchae may be a more appropriate location for tVNS therapy in the auricle than the ear canal and inner tragus, because stimulation of this location resulted in the strongest activation of vagal afferent pathway in the brainstem. Although further studies on the long-term effects of tVNS are necessary, the present findings represent an initial step toward the design of an optimal methodology for tVNS treatment that can be a noninvasive alternative to direct VNS.

Authorship Statement

Dr. Yakunina conducted the study, including subject recruitment, data collection, and data analysis, and wrote the manuscript. Dr. Nam designed the study, designed the electrical stimulator and funded its development, recruited subjects, supervised data collection and analysis, and provided important input and insights in writing the manuscript. Dr. Kim provided materials for the experiment and help in recruiting the subjects. All authors read and approved the final version of the manuscript.

How to Cite this Article:

Yakunina N., Kim S.S., Nam E.-C. 2016. Optimization of Transcutaneous Vagus Nerve Stimulation Using Functional MRI.
Neuromodulation 2016; E-pub ahead of print. DOI: 10.1111/ner.12541

REFERENCES

1. Klein HU, Ferrari GM. Vagus nerve stimulation: a new approach to reduce heart failure. *Cardiol J* 2010;17:638–644.
2. Schachter SC, Saper CB. Vagus nerve stimulation. *Epilepsia* 1998;39:677–686.
3. Milby AH, Halpern CH, Baltuch GH. Vagus nerve stimulation for epilepsy and depression. *Neurotherapeutics* 2008;5:75–85.
4. Groves DA, Brown VJ. Vagal nerve stimulation: a review of its applications and potential mechanisms that mediate its clinical effects. *Neurosci Biobehav Rev* 2005; 29:493–500.
5. George MS, Ward HE, Jr, Ninan PT et al. A pilot study of vagus nerve stimulation (VNS) for treatment-resistant anxiety disorders. *Brain Stimul* 2008;1:112–121.
6. Seol GH, Ziburkus J, Huang S et al. Neuromodulators control the polarity of spike-timing-dependent synaptic plasticity. *Neuron* 2007;55:919–929.
7. Dorr AE, Debonnel G. Effect of vagus nerve stimulation on serotonergic and noradrenergic transmission. *J Pharmacol Exp Ther* 2006;318:890–898.

8. Hays SA, Rennaker RL, Kilgard MP. Targeting plasticity with vagus nerve stimulation to treat neurological disease. *Prog Brain Res* 2013;207:275–299.
9. Pena DF, Childs JE, Willett S, Vital A, McIntyre CK, Kroener S. Vagus nerve stimulation enhances extinction of conditioned fear and modulates plasticity in the pathway from the ventromedial prefrontal cortex to the amygdala. *Front Behav Neurosci* 2014;8:327.
10. Porter BA, Khodaparast N, Fayyaz T et al. Repeatedly pairing vagus nerve stimulation with a movement reorganizes primary motor cortex. *Cereb Cortex* 2012;22: 2365–2374.
11. Engineer ND, Riley JR, Seale JD et al. Reversing pathological neural activity using targeted plasticity. *Nature* 2011;470:101–104.
12. Lulic D, Ahmadian A, Baaj AA, Benbadis SR, Vale FL. Vagus nerve stimulation. *Neurosurg Focus* 2009;27:E5.
13. Nemeroff CB, Mayberg HS, Krahl SE et al. VNS therapy in treatment-resistant depression: clinical evidence and putative neurobiological mechanisms. *Neuropsychopharmacology* 2006;31:1345–1355.
14. Bonaz B, Picq C, Sinniger V, Mayol JF, Clarencon D. Vagus nerve stimulation: from epilepsy to the cholinergic anti-inflammatory pathway. *Neurogastroenterol Motil* 2013;25:208–221.
15. Ellrich J. Transcutaneous vagus nerve stimulation. *Eur Neurol Rev* 2011;6:254–256.
16. Kraus T, Hosl K, Kiess O, Schanze A, Kornhuber J, Forster C. BOLD fMRI deactivation of limbic and temporal brain structures and mood enhancing effect by transcutaneous vagus nerve stimulation. *J Neural Transm (Vienna)* 2007;114:1485–1493.
17. Kraus T, Kiess O, Hosl K, Terekhin P, Kornhuber J, Forster C. CNS BOLD fMRI effects of sham-controlled transcutaneous electrical nerve stimulation in the left outer auditory canal—a pilot study. *Brain Stimul* 2013;6:798–804.
18. Dietrich S, Smith J, Scherzinger C et al. A novel transcutaneous vagus nerve stimulation leads to brainstem and cerebral activations measured by functional MRI. *Biomed Tech (Berl)* 2008;53:104–111.
19. Frangos E, Ellrich J, Komisaruk BR. Non-invasive access to the vagus nerve central projections via electrical stimulation of the external ear: fMRI evidence in humans. *Brain Stimul* 2015;8:624–636.
20. Krahl SE, Clark KB. Vagus nerve stimulation for epilepsy: a review of central mechanisms. *Surg Neurol Int* 2012;3:S255–S259.
21. Peuker ET, Filler TJ. The nerve supply of the human auricle. *Clin Anat* 2002;15:35–37.
22. Tekdemir I, Aslan A, Elhan A. A clinico-anatomic study of the auricular branch of the vagus nerve and Arnold's ear-cough reflex. *Surg Radiol Anat* 1998;20:253–257.
23. Kiyokawa J, Yamaguchi K, Okada R, Maehara T, Akita K. Origin, course and distribution of the nerves to the posterosuperior wall of the external acoustic meatus. *Anat Sci Int* 2014;89:238–245.
24. Alvord LS, Farmer BL. Anatomy and orientation of the human external ear. *J Am Acad Audiol* 1997;8:383–390.
25. Lomarev M, Denslow S, Nahas Z, Chae JH, George MS, Bohning DE. Vagus nerve stimulation (VNS) synchronized BOLD fMRI suggests that VNS in depressed adults has frequency/dose dependent effects. *J Psychiatr Res* 2002;36:219–227.
26. Magdaleno-Madrigal VM, Valdes-Cruz A, Martinez-Vargas D et al. Effect of electrical stimulation of the nucleus of the solitary tract on the development of electrical amygdaloid kindling in the cat. *Epilepsia* 2002;43:964–969.
27. Groves DA, Bowman EM, Brown VJ. Recordings from the rat locus coeruleus during acute vagal nerve stimulation in the anaesthetised rat. *Neurosci Lett* 2005;379:174–179.
28. Van Bockstaele EJ, Peoples J, Telegan P. Efferent projections of the nucleus of the solitary tract to peri-locus coeruleus dendrites in rat brain: evidence for a monosynaptic pathway. *J Comp Neurol* 1999;412:410–428.
29. Keren NI, Lozar CT, Harris KC, Morgan PS, Eckert MA. In vivo mapping of the human locus coeruleus. *Neuroimage* 2009;47:1261–1267.
30. Bradley RM, *The role of the nucleus of the solitary tract in gustatory processing*. Boca Raton, FL: CRC Press/Taylor & Francis, 2006.
31. Naidich T, Duvernoy H, Delman B, Sorensen A, Kollias S, Haacke E. *Duvernoy's atlas of the human brain stem and cerebellum*. Vienna: Springer, 2009.
32. Bohning DE, Lomarev MP, Denslow S, Nahas Z, Shastri A, George MS. Feasibility of vagus nerve stimulation-synchronized blood oxygenation level-dependent functional MRI. *Invest Radiol* 2001;36:470–479.
33. Chae JH, Nahas Z, Lomarev M et al. A review of functional neuroimaging studies of vagus nerve stimulation (VNS). *J Psychiatr Res* 2003;37:443–455.
34. Narayanan JT, Watts R, Haddad N, Labar DR, Li PM, Filippi CG. Cerebral activation during vagus nerve stimulation: a functional MR study. *Epilepsia* 2002;43: 1509–1514.
35. Nahas Z, Teneback C, Chae JH et al. Serial vagus nerve stimulation functional MRI in treatment-resistant depression. *Neuropsychopharmacology* 2007;32: 1649–1660.
36. Sucholeiki R, Alsaadi TM, Morris GL, 3rd, Ulmer JL, Biswal B, Mueller WM. fMRI in patients implanted with a vagal nerve stimulator. *Seizure* 2002;11:157–162.
37. Krahl SE, Clark KB, Smith DC, Browning RA. Locus coeruleus lesions suppress the seizure-attenuating effects of vagus nerve stimulation. *Epilepsia* 1998;39: 709–714.
38. Fornai F, Ruffoli R, Giorgi FS, Paparelli A. The role of locus coeruleus in the antiepileptic activity induced by vagus nerve stimulation. *Eur J Neurosci* 2011;33:2169–2178.
39. Poncelet BP, Wedeen VJ, Weisskoff RM, Cohen MS. Brain parenchyma motion: measurement with cine echo-planar MR imaging. *Radiology* 1992;185:645–651.
40. Barnes A, Duncan R, Chisholm JA, Lindsay K, Patterson J, Wyper D. Investigation into the mechanisms of vagus nerve stimulation for the treatment of intractable epilepsy, using 99mTc-HMPAO SPET brain images. *Eur J Nucl Med Mol Imaging* 2003; 30:301–305.
41. Van Laere K, Vonck K, Boon P, Brans B, Vandekerckhove T, Dierckx R. Vagus nerve stimulation in refractory epilepsy: SPECT activation study. *J Nucl Med* 2000;41:1145–1154.
42. Henry TR, Bakay RA, Pennell PB, Epstein CM, Votaw JR. Brain blood-flow alterations induced by therapeutic vagus nerve stimulation in partial epilepsy: II. prolonged effects at high and low levels of stimulation. *Epilepsia* 2004;45:1064–1070.
43. Zobel A, Joe A, Freymann N et al. Changes in regional cerebral blood flow by therapeutic vagus nerve stimulation in depression: an exploratory approach. *Psychiatry Res* 2005;139:165–179.
44. Henry TR, Bakay RA, Votaw JR et al. Brain blood flow alterations induced by therapeutic vagus nerve stimulation in partial epilepsy: I. acute effects at high and low levels of stimulation. *Epilepsia* 1998;39:983–990.
45. Kirsch DL, Nichols F. Cranial electrotherapy stimulation for treatment of anxiety, depression, and insomnia. *Psychiatr Clin North Am* 2013;36:169–176.
46. Gilula MF, Kirsch DL. Cranial electrotherapy stimulation review: a safer alternative to psychopharmaceuticals in the treatment of depression. *J Neurother* 2005;9:7–26.
47. Madden R, Kirsch DL. Low intensity transcranial electrostimulation improves human learning of a psychomotor task. *Am J Electromed* 1987;2:41–45.
48. Feusner JD, Madsen S, Moody TD et al. Effects of cranial electrotherapy stimulation on resting state brain activity. *Brain Behav* 2012;2:211–220.
49. Lehtimaki J, Hyvarinen P, Ylikoski M et al. Transcutaneous vagus nerve stimulation in tinnitus: a pilot study. *Acta Otolaryngol* 2013;133:378–382.
50. Young ED, Nelken I, Conley RA. Somatosensory effects on neurons in dorsal cochlear nucleus. *J Neurophysiol* 1995;73:743–765.
51. Levine RA, Nam EC, Oron Y, Melcher JR. Evidence for a tinnitus subgroup responsive to somatosensory based treatment modalities. *Prog Brain Res* 2007;166:195–207.
52. Wright DD, Ryugo DK. Mossy fiber projections from the cuneate nucleus to the cochlear nucleus in the rat. *J Comp Neurol* 1996;365:159.
53. Dehmel S, Cui YL, Shore SE. Cross-modal interactions of auditory and somatic inputs in the brainstem and midbrain and their imbalance in tinnitus and deafness. *Am J Audiol* 2008;17:S193–S209.
54. Kanold PO, Davis KA, Young ED. Somatosensory context alters auditory responses in the cochlear nucleus. *J Neurophysiol* 2011;105:1063–1070.
55. Koehler SD, Pradhan S, Manis PB, Shore SE. Somatosensory inputs modify auditory spike timing in dorsal cochlear nucleus principal cells. *Eur J Neurosci* 2011;33:409–420.
56. Shore SE. Plasticity of somatosensory inputs to the cochlear nucleus–implications for tinnitus. *Hear Res* 2011;281:38–46.
57. Shore SE, Zhou J. Somatosensory influence on the cochlear nucleus and beyond. *Hear Res* 2006;216–217:90–99.
58. Levine RA. Somatic (craniocervical) tinnitus and the dorsal cochlear nucleus hypothesis. *Am J Otolaryngol* 1999;20:351–362.

